Remediation of Ni^{2+} in a nickel-contaminated water sample using magnetic nanoprobes prepared via green process by *Psidium guajava* leaves extract

IOP Conf. Series: Earth and Environmental Science **277** (2019) 012033 doi:10.1088/1755-1315/277/1/012033

Remediation of Ni^{2+} in a nickel-contaminated water sample using magnetic nanoprobes prepared via green process by *Psidium guajava* leaves extract

R Y Capangpangan[1,2,3,*], M J B Corpuz[4] and A C Alguno[5]

[1] Chemistry Division, Caraga State University, Philippines
[2] Mineral Resources Management Research and Training Center (MinRes)
[3] Material Science and Polymer Chemistry Laboratory, Caraga State University
[4] Environmental Science Division, Caraga State University, Philippines
[5] Department of Physics, MSU-Iligan Institute of Technology (MSU-IIT), Philippines

[*]E-mail: rycapangpangan@carsu.edu.ph

Abstract. Rapid detection of toxic metal ions is of paramount importance in environmental studies for efficient environmental remediation. The use of effective nanomaterials that facilitate fast detection and cost-effective analysis is one of the active areas of research nowadays. Plant-based magnetic nanoparticles (MNPs) were prepared via a reverse chemical co-precipitation method using guava leaves extract as a reducing agent. The prepared MNPs were utilized as an adsorbent for the remediation of Ni^{2+} ions in aqueous solution. Batch adsorption experiment was conducted to evaluate the amount of Ni^{2+} ions being adsorbed in the surface of the MNPs. Results revealed that 98% of the Ni^{2+} ions were adsorbed in the surface of the MNPs when 5.0 mg of the MNP adsorbent was utilized. Likewise, it was observed that the maximum adsorption was achieved even at 10 minutes incubation time using 1.597 ppm initial Ni^{2+} concentration and the use of 5.0 mg of MNP. The adsorption behavior and mechanism of MNPs as the adsorbent is probably dominated by electron-electron interaction, and the data can be correlated with the functional group analysis using Fourier-Transform Infrared Spectroscopy (FT-IR). It was also observed that higher adsorption capacity (~8.5 mg/g) was attained when 5.0 mg of MNP was used. Importantly, the equilibrium data perfectly fit in the Langmuir isotherm with a slight deviation in the Freundlich isotherm.

1. Introduction

Designing and exploration of new green synthetic strategies for the synthesis of magnetic nanoparticles is one of the growing areas of science [1,2]. In spite of its success for the synthesis and preparation of magnetic nanoparticles, there is still a rising concern on the application of green synthesis for the preparation of magnetic nanoparticles. The main objective of the development of a green strategy for the preparation of magnetic nanoparticles is to offer a safe, non-toxic, easy and environment-friendly technique [3]. Biosynthesis of magnetic nanoparticles often possesses many advantages over other chemical methods, as the former method offers an environment-friendly protocol and the diverse potential sources of biological entities [4]. Many reports have been published on the use of plant-based materials for the production of magnetic nanoparticles due to the rich biodiversity and easy availability of the different plant materials [5,6]. It has also been reported that the biologically-synthesized nanomaterials have potential applications in various areas such as treatment, diagnosis, targeted drug

delivery, development of surgical nano-devices and for commercial product manufacturing. In addition, biologically-synthesized magnetic nanoparticles, particularly Fe_3O_4 nanoparticles were also utilized for environmental remediation purposes [7-9].

Even though plant-based magnetic nanoparticles were previously prepared, however, few reports were published on the utilization of guava leaves extract for the synthesis of magnetic nanoparticles. Guava leaves extract has been used as a capping ligand and a stabilizing agent in the preparation of silver nanoparticles [10,11], copper nanoparticles [12] and other metallic oxide nanoparticles [13,14]. Also, guava leaves extract was reported to be the stabilizing ligand in the preparation of hematite (Fe_2O_3). Having these biosynthesized nanomaterials being prepared, however, their applications towards environmental remediation is limited. In this particular study, the biosynthesized magnetic nanoparticles were utilized as nanoprobes in remediating Ni^{2+} from the Ni-contaminated water.

Nickel is one of the many trace metals that is widely distributed in the environment [15]. It occurs naturally in soil and surface water with a concentration lower than 100 and 0.005 ppm, respectively [16]. Nickel pollution is prevalent mostly in developing countries. In the Philippines, heavy metal contamination from mining is inevitable, particularly nickel contamination. Mining activities, both large-scale and small-scale mining are prevalent in Caraga Region, where it is dubbed as the mining hotspot and the nickel capital of the country [17]. Hence, an active monitoring and effective remediation programs have to be implemented. Also, it is imperative to develop an analytical strategy for a fast and sensitive platform for nickel detection. However, the common method for heavy metal determination often involves a labor-intensive process of sample preparation, more expensive techniques and is not readily available for on-site and rapid screening of environmental samples. Likewise, in most cases where the target analytes are in a minute concentration, prior sample pre-concentration is necessary to detect the target analyte. Hence, such analysis requires a laborious and time-consuming process before obtaining the desired results.

To address this particular concern, analytical methodologies such that prior sample pre-concentration can be avoided are highly required. The use of a certain probe which can act as "bait" to where the metal ion of interest can interact is normally used. Several reports have been reported that nano-based materials have been used for enrichment of metal ions [18]. Most often, these nanoprobes were prepared via a chemically synthetic process and functionalized with the target functional groups depending on the desired applications. The applications of these nanoprobes have been successfully demonstrated; however, complexity arises during the isolation of nanoprobes from a complex sample mixture. Thus, nanoprobes which can be collected and isolated easily are highly desirable, such as the use of magnetic nanoprobes. Magnetic nanoparticles offer an advantage over other particles as the former can be easily manipulated by the application of an external magnetic field. Importantly, the in-depth application of magnetic nanoparticles for wastewater applications as an enrichment material is not widely studied; hence, this study is conducted. Likewise, this study promotes the use and production of recyclable materials for effective and efficient sequestration and further detoxification of hazardous contaminants present in the mining wastewater to avoid further contamination in the environment.

2. Materials and Methods

2.1. Materials

Ferric chloride hexahydrate ($FeCl_3 \cdot 6H_2O$, Scharlau), iron (II) sulfate heptahydrate ($FeSO_4.7H_2O$, APS Ajax Finechem), sodium hydroxide (Scharlau), and hydrochloric acid (Merck) were used as received. Guava leaves were collected from Barangay Ampayon, Butuan City and air-dried in the CSU Laboratory. Metal ion concentration was evaluated using Flame Atomic Absorption Spectrometer (Flame-AAS). All the chemicals and reagents were used as received.

2.2. Preparation of guava leaves extract

The guava leaves extract was obtained through decoction method. Briefly, mature guava leaves were washed 2x (twice) with tap water, then with distilled (2x) water to make sure that the leaves were free

of dirt and other contaminants. Then, the leaves were cut into pieces and boiled in the beaker (500 mL) for an hour. The leaves were then filtered and stored in a clean container.

2.3. Synthesis of magnetic nanoparticles

Magnetic nanoparticles (MNPs) were prepared via reverse co-precipitation method. Briefly, 2.7 g of ferric chloride hexahydrate ($FeCl_3 \cdot 6H_2O$) and 1.4 g of iron sulfate heptahydrate ($FeSO_4.7H_2O$) were dissolved in 10 mL of the freshly prepared Guava leaves extract with continuous stirring until complete dissolution. The resulting mixture was then added dropwise to the10 mL of distilled water containing 2 mL of 1.0 M NaOH with constant stirring. The resulting MNPs were being washed with distilled water, stored in a clean container and stored in the 4°C environment if not in use.

2.4. Characterization

Characterization techniques were employed to evaluate the surface morphology of the prepared MNPs. To evaluate the different functional groups present in the sample, FT-IR analysis was conducted. Characterization techniques such as the Transmission Electron Microscopy (TEM), was used to determine the particle size and surface morphology and elemental analysis using Energy Dispersive X-ray Analysis (EDX).

2.5. Adsorption experiment

Batch adsorption experiments for Ni^{2+} ion adsorption by magnetic nanoparticles were initially conducted at a fixed temperature (room temperature) and a known standard Ni^{2+}concentration. In brief, 5.00 mg of the prepared MNPs was added to 50 mL of known concentration (1.597 mg/L) of Ni^{2+} ions and was allowed to equilibrate for 10 minutes by shaking it using Orbital shaker at 240 rpm. At the end of 10 minutes, the mixture was filtered, and the concentration of Ni^{2+} in the filtrate was analyzed using Flame AAS. The adsorption or removal efficiency was then evaluated using the equation:

$$\text{Adsorption Efficiency (\%)} = \frac{C_0 - C_e}{C_0} \text{ x } 100$$

where C_0 is the initial concentration and C_e is the final (equilibrium) concentration. Further optimization was carried out; variation of the adsorbent amount, nickel concentration, and time of incubation. Removal efficiency was then evaluated using the same equation as described above.

2.5.1. Effect of contact time. A pre-determined amount of MNPs was thoroughly mixed with a known concentration of nickel solution (50 mL) at a fixed (room) temperature. The mixture was then shaken (at 240 rpm) at different time intervals: 10, 30, 60, 90 and 120 minutes. After shaking (at the desired time), the mixture was then filtered, and the concentration of Ni^{2+} in the filtrate was checked by Flame-AAS.

2.5.2. Effect of MNP amount. The influence of MNP amount to the adsorption efficiency was investigated by conducting the adsorption experiment at a different dosage of the adsorbent (MP). Different MNP amount, e.g., 5.0, 10, 15, 20 and 25 mg were used in equilibrating with a known concentration (1.5 mg/L) of Ni^{2+} at the optimized time (as described in 2.5.1 above). The concentration of Ni^{2+} in the filtrate (after filtration) was then evaluated using Flame-AAS.

2.5.3. Effect of standard Nickel concentration. Different Ni^{2+} concentration (0.5, 1.5, 2.0, 5.0, 10, 20 and 50 mg/L) were equilibrated with a fixed MNP amount (as described in 2.5.2 above) and time (as described in 2.5.1 above). Then, the concentration that remains in the filtrate was determined using Flame-AAS.

2.6. Equilibrium Isotherms

Equilibrium isotherms were measured to determine the adsorption capacity of the adsorbent for Ni^{2+} ions. The most common types of models defining this type of system are the Langmuir and Freundlich models. The adsorption capacity q_e (mg/g) after equilibrium was calculated by a mass balance relationship equation as follows:

$$q_e = \frac{(C_0 - C_e)\,V}{W}$$

where C_0 is the initial concentration, C_e is the equilibrium (final) concentration, V is the volume of the sample used (L) and W is the mass of the MNP used (g).

3. Results and discussion

3.1. Nanoparticle characterization

Transmission Electron Microscopy (TEM) and Scanning Electron Microscopy (SEM) were used to investigate the size and surface morphology of the synthesized magnetic nanoparticles (MNPs).

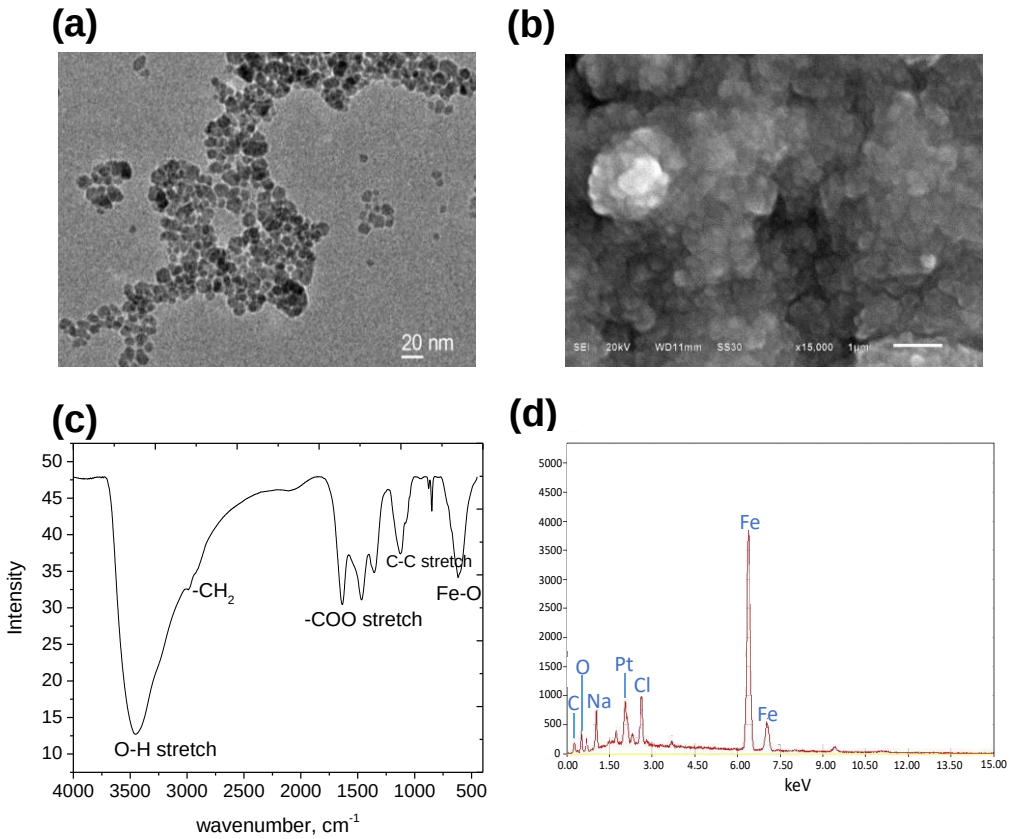

Figure 1. (a) TEM image, (b) SEM image, (c) FT-IR spectra and the EDX spectra of the synthesized magnetic nanoparticles.

As shown, the size of the individual magnetic nanoparticles based on the TEM analysis (Figure 1a) ranging within 10-17 nm, and the SEM result (Figure 1b) suggests that the nanoparticles tend to form aggregates. Likewise, the EDX analysis (Figure 1d) suggests that Fe, O, Pt and C are the main constituents of the magnetic nanoparticles with traces of Na and Cl. On the other hand, FT-IR spectra (Figure 1c) shows a strong signal at 3450 cm^{-1} which is a characteristic peak for –OH stretching. Also,

the absorption band at 500 cm^{-1} can be assigned to Fe-O (from the iron oxide nanoparticles) signal. The peak at ~1250 cm^{-1} correspond to –C-C- stretch, 2920 cm^{-1} for aromatic $–CH_2$ and peak at 1560 cm^{-1} is a characteristic peak for COO- stretch. Based on these assignments, it can be deduced that the surface of the magnetic nanoparticles is covered with an OH-rich functional groups. Hence, it is speculated that the surface of the nanoparticles is fully functionalized with tannins and other related functional groups such as flavonoids. Guava leaves are reported to be of the high amount of tannins and flavonoids [19] which can bind/chelate heavy metal ions [20].

3.2. Adsorption experiment

In the initial experiment, 20 mg of MNP was equilibrated at room temperature with 1.5 ppm standard Ni^{2+} solution for 60 minutes. After the specified time, the concentration of Ni^{2+} that remains in the filtrates was measured. The result shows that using the pre-set experimental condition; higher adsorption efficiency was recorded (98%). Prompted by the obtained data, the optimization of the experimental parameters was conducted.

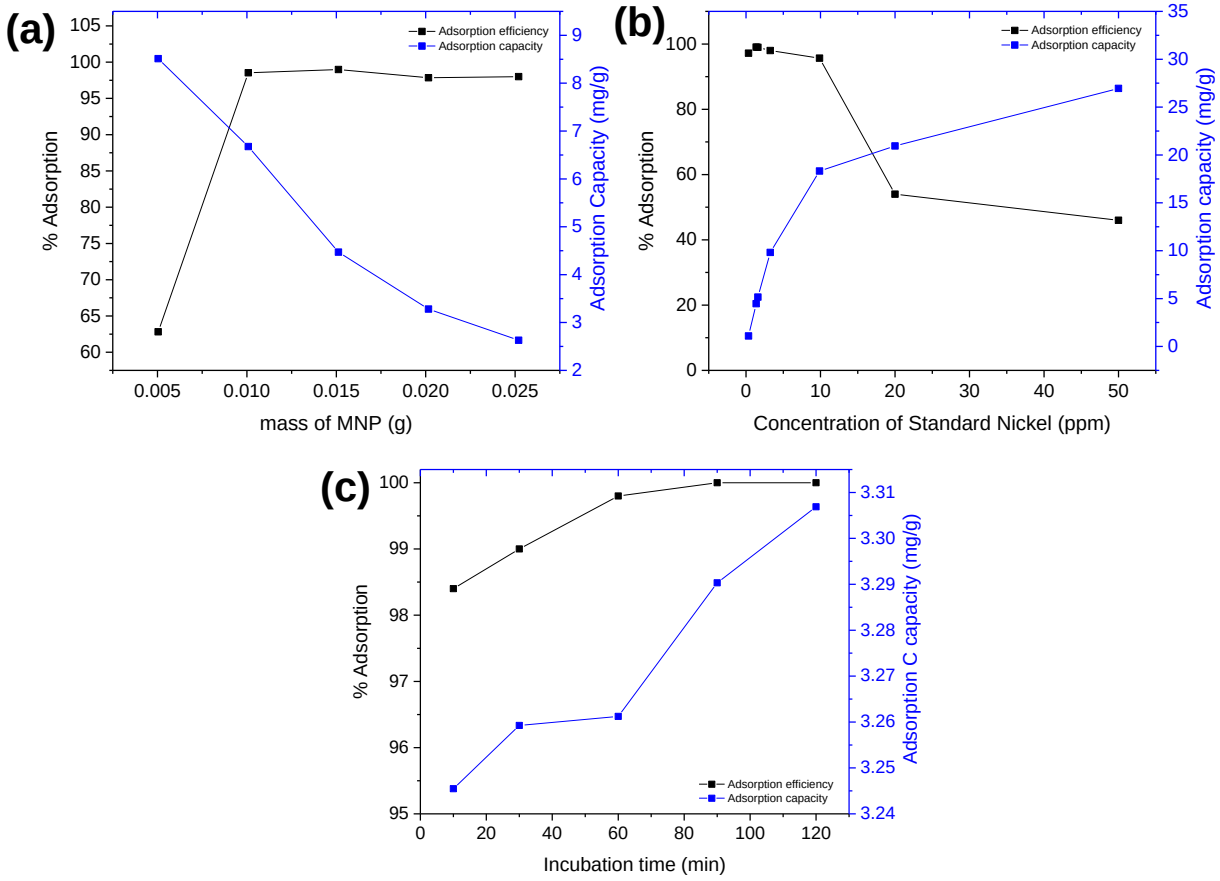

Figure 2. Graphical representation on the effect of the different parameters (a) MNP amount, (b) concentration of Ni^{2+} standard solution, and (c) incubation time on the adsorption efficiency for Ni^{2+} removal (black line) and on the adsorption capacity of the MNP in mg/g (blue line).

3.2.1. Effect of MNP amount. The effect of MNP amount to the adsorption performance of the nanoparticles as adsorbent was evaluated. In this particular study, various MNP amounts were used: 5.0, 10.0, 15.0, 20.0 and 25.00 mg. Equilibration time with 1.5 mg/L of Ni^{2+} solution was fixed at 60 minutes prior to the measurement of Ni^{2+} ions that was adsorbed in the nanoadsorbents. Results showed (Figure 2a) that maximum adsorption efficiency (98%) was obtained when 15.0 mg of MNP was used. It is

being observed further that increasing the MNP amount do not show any significant changes in the amount of Ni^{2+} ions being adsorbed (%adsorption) on the surface of MNPs. Although there was a rapid increase in the percent adsorption when 5.0, 10.0 and 15.0 mg of MNP was used; however, the further increase in the MNP amount greater than 15.0 mg does not have any significant enhancement in the percent adsorption value. Plausibly, this is because of the saturation of the adsorption sites of the magnetic nanoparticles, that is 15.0 mg of the MNP is the optimum adsorbent dosage amount that has the highest adsorption efficiency at a given concentration of Ni^{2+} (1.5 mg/L).

Furthermore, the figure (Figure 2a) shows that there is an inverse relationship between the MNP amount and the adsorption capacity. It is reflected in the figure that lowest adsorption capacity was attained when 25 mg of MNP was used, while highest adsorption capacity (~8.5 mg/g) was recorded when 5 mg of MNP was used. The result suggests that an increase in the amount of adsorbent, there is a corresponding decrease in the adsorption capacity. The observed relationships between the adsorbent amount and the adsorption capacity of the MNP can be probably due to the aggregation of the adsorbent that consequently leads to a decrease in the available adsorption sites. Moreover, it is also possible that during the process, heterogeneous distribution of the active adsorption sites of the MNPs happens as the amount of the adsorbent increase, thus, decreases the availability of the other sites for Ni^{2+} adsorption [21].

3.2.2. Effect of standard nickel concentration. The effect of Ni^{2+} concentration on the percent adsorption was further investigated. As noted, the initial metal ion concentration has a significant effect on their removal from aqueous solutions [22]. As shown in Figure 2b, it was observed that the % adsorption decreases as the concentration of Ni^{2+} increases. The adsorption of Ni^{2+} in the surface of MNPs showed a noticeable decrease (from 99% to 46%) from 0.5 to 50 mg/L initial Ni^{2+} concentration. This observation corroborates to other reported literature [23], wherein the observed results can be plausibly explained based on the fact that the availability of the adsorption sites on the surface of MNPs is a function of initial metal ion concentration. Sufficient adsorption sites are available at lower initial concentrations, but at higher concentrations, the metal ions exist in greater proportion than the adsorption sites. As the exterior surface became exhausted, the adsorbate uptake rate began to decrease [24]. Thus, it can be deduced that the removal of Ni^{2+} ion is mainly concentration-dependent using the magnetic nanoparticles adsorbent.

Similarly, the figure (Figure 2b, blue line) shows the effect of initial Ni^{2+} concentration on the adsorption capacity of MNPs. The plot reveals that the MNPs adsorption capacity increases from 1.095 mg/g to 18.32 mg/g as the concentration of Ni^{2+} increases from 0.5 to 10 mg/L. It is also notable, moreover that there is a slight decrease (15.94 mg/g) in the adsorption capacity value of MNP at 20 mg/L Ni^{2+} concentration. However, relatively higher adsorption capacity (26.95 mg/g) is observed at a highest Ni^{2+} concentration (50 mg/L). Most likely, the observed increase of adsorption capacity is due to the increase in initial concentrations as it resulted in higher mass gradient pressures between the aqueous solution and nanoparticle. It can also be reasoned out that a large amount of force is needed to overcome the mass transfer resistance between the aqueous solution and solid phase [24].

3.2.3. Effect of incubation time. In principle, the efficiency of metal ion adsorption strongly depends on the time of adsorption. To determine the effect of contact time on the percent adsorption, a fixed amount of MNP (5.0 mg) and fixed Ni^{2+} concentration (1.597 mg/L) was incubated in different time intervals. As shown, higher % adsorption (98.7%) was observed for MNPs incubated at 10 minutes. Increasing the time of incubation do not show any significant difference in terms of percent adsorption, 99% and 99.8% for 30 minutes and 60 minutes of incubation time, respectively. A 100 % adsorption was attained when the incubation time was increased further for up to 120 minutes. Surprisingly, higher percent adsorption was obtained even after 10 minutes of incubation (98.7%). This result suggests that MNP as the adsorbent is an excellent material for remediation of Ni^{2+} as it will not require a longer time to remove almost all of the Ni^{2+} ions in aqueous solution. The metal removal rate at the initial contact time was high, which could be attributed to a large number of vacant binding sites available for metal ion

adsorption to the nanoparticles surfaces [24]. Several reports have been documented on the use of MNP as an adsorbent for different heavy metal ions [25,26]. Although they reported excellent adsorption capacity of the MPs, however, longer incubation time is required. The MNPs adsorption capacity (mg/g) was evaluated to check the performance of MNPs as an adsorbent for Ni^{2+} ions. As shown in Figure 2c, it is notable that there is an increase in the adsorption capacity as the incubation time becomes longer.

3.2.4. Sequestration of Ni^{2+} in real wastewater sample using the synthesized magnetic nanoprobes.

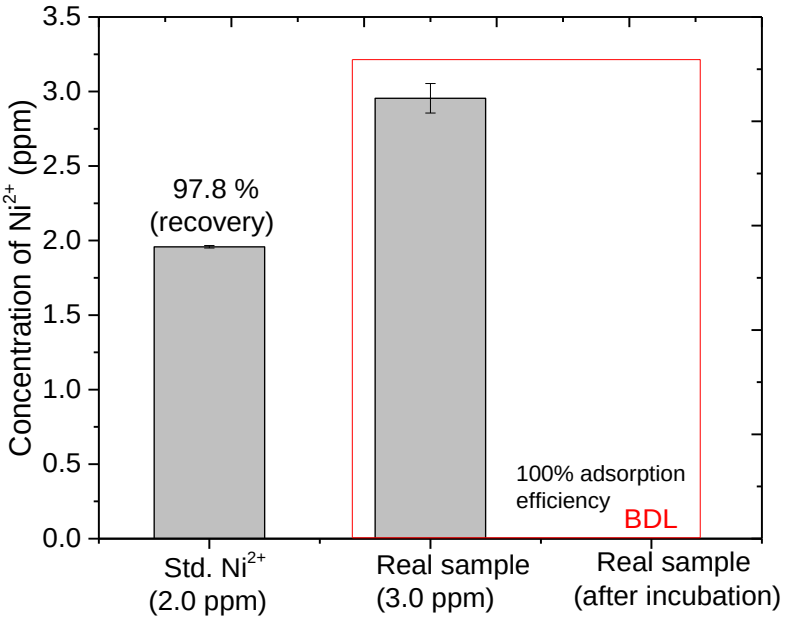

Figure 3. Application of the synthesized magnetic nanoprobes in the sequestration of Ni^{2+} from real wastewater sample.
Note: BDL – Below detection limit

Inspired by the obtained results using the standard Ni^{2+} solution, the synthesized magnetic nanoprobes were utilized in the sequestration of Ni^{2+} from the real wastewater sample. The magnetic nanoprobes (~10 mg) was incubated in the wastewater sample for 120 minutes. Then, the samples were filtered prior to AAS measurement. It is noteworthy, moreover that the percent recovery was determined to ensure the reliability of the measurement. As shown (Figure 3), a higher % recovery was obtained using the 2.0 ppm Ni^{2+} solution (~97.8%). The Ni^{2+} concentration in the wastewater sample was determined by AAS and is equal to 2.95 ± 0.0986 ppm. As noted, after incubation of the magnetic nanoprobes, the Ni^{2+} concentration was not detected, which simply implies that all the Ni^{2+} (100% adsorption) were adsorbed in the surface of the magnetic nanoprobes.

3.2.5. Adsorption isotherm. As reported, adsorption is a physical-chemical process that the mass transfers a solute (adsorbate) from the fluid phase to the adsorbent surface [27]. Adsorption of metal ions can be described by various adsorption kinetic models. Among the many adsorption isotherms used to model the amount of solute adsorbed per unit of adsorbent as a function of equilibrium concentration in the bulk solution, Freundlich and Langmuir's isotherms were commonly evaluated. In this particular study, data were fitted to both Langmuir and Freundlich isotherms. The adsorption isotherms were obtained at optimum conditions of metal ion adsorption for the prepared adsorbent.

3.2.5.1 Freundlich adsorption isotherm. Figure 4a shows the plot of Freundlich adsorption isotherm. The isotherm assumes that the surface sites of the adsorbent have different binding energies and has the following form:

$$\log q_e = \log k_F + \frac{1}{n}\log C_e$$

where k_F, represents the adsorption capacity when metal ion equilibrium concentration equals to 1 (mg/g) and n is the degree of independence of adsorption with equilibrium concentration. Freundlich parameters are shown in Table 1. The high R^2 values obtained are shown in the table.

Table 1. Isotherm constants of Langmuir and Freundlich models for Ni^{2+} remediation using magnetic particles.

Adsorbent	Langmuir Constants			Freundlich Constants		
	q_m(mg/g)	k_L(L/mg)	R^2	k_f	n	R^2
MNP	48.45	0.0677	0.99692	0.4692	1.249	0.98477

Based on the reported criteria [28], the obtained results (n = 1.249) indicates that the adsorption process of Ni^{2+} to the surface of the MNP is beneficial or favorable adsorption. Also, the obtained n value provides an adequate description of the adsorption process over a restricted range of analyte concentration. The 1/n value of 0.8006 (less than 1) indicates that significant adsorption takes place at low concentration, but the increase in the amount adsorbed with concentration becomes less significant at higher concentration.

3.2.5.2 Langmuir adsorption isotherm. The Langmuir isotherm assumes monolayer coverage of the adsorption surface and no subsequent interaction among adsorbed molecules. Thus, the adsorption saturates, and no further adsorption can occur. The isotherm can be represented in linear form by the following equation:

$$\frac{1}{q_e} = \left(\frac{1}{q_m k_L}\right).\left(\frac{1}{C_e}\right) + \frac{1}{q_m}$$

where C_e is the equilibrium concentration of metal ions in solution (mg/L), q_e is the amount of metal ion adsorbed on adsorbents (mg/g), and q_m and k_L are the monolayer adsorption capacity (mg/g) and Langmuir equilibrium constant (L/mg) which indicates the nature of adsorption, correspondingly. The values of q_m and k_L were determined graphically. A plot of $\frac{1}{q_e}$ versus $\frac{1}{C_e}$ gives a straight line of slope equal to $\frac{1}{q_m k_L}$ and the intercept is $\frac{1}{q_m}$ which corresponds to complete monolayer coverage. The adherence of adsorption data to Langmuir equation was the the tested and the results are shown in Table 1.

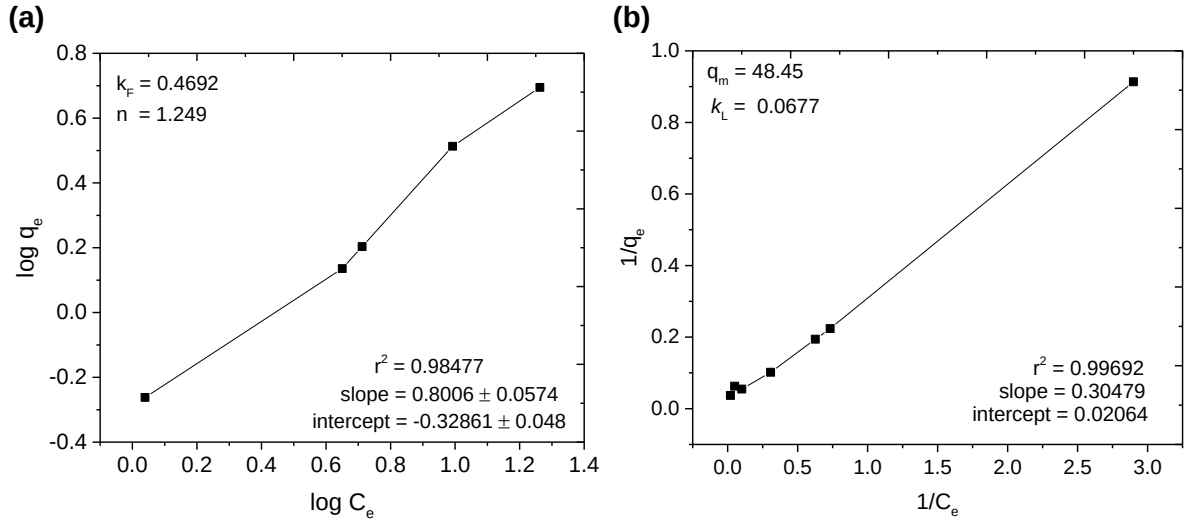

Figure 4. The plot of fitted data using (a) Freundlich isotherm and (b) Langmuir isotherm for metal adsorption by the synthesized magnetic nanoparticles.

Figure 4b shows the fitted data to Langmuir isotherm. As can be seen, experimental data were better fitted to the Langmuir equation than that of the Freundlich isotherm. The result suggests that the sorption process of Ni^{2+} on the surface of the magnetic nanoparticles follows the Langmuir isotherm model, where Ni^{2+} ions were taken up independently on a single type of binding site in such a way that the uptake of the first metal ion does not affect the sorption of the next ion. The results also indicate that the heterogeneous distribution of active sites on the surface of the adsorbents occurs.

4. Conclusions and recommendation

Effective magnetic nanoprobe as Ni^{2+} adsorbent has been synthesized via the green process. The adsorbent material used is the plant-based magnetic nanoparticles (MNPs) prepared by reverse chemical co-precipitation method. Batch adsorption experiment was conducted to evaluate the effectiveness of MNPs for the remediation of Ni^{2+} ions. Different parameters such as Ni^{2+} standard concentration, incubation time and MNP dosage were studied at ambient temperature. Results showed that 98.5% of the Ni^{2+} ions were adsorbed on the surface of MNPs when 10 mg of the MNP adsorbent was used. Likewise, the optimum equilibration time with the maximum percent adsorption was attained at 60 minutes, although relatively higher adsorption was observed even at 10 minutes incubation period. Similarly, maximum adsorption efficiency was also attained using 10 mg of the adsorbent. Also, it was observed that higher adsorption capacity (~8.5 mg/g) was attained when 5.0 mg of MNP was used. The adsorption behavior and mechanism of MNPs can be correlated with the functional group analysis (FT-IR). The result shows that the binding mechanism of the MNPs with Ni^{2+} ions is most probably dominated by electron-electron interaction via OH functional group. FT-IR data revealed that the surface of MNPs are covered with protruding OH functional group as there is a sharp and distinct band at 3450 cm^{-1} which can be assigned to –OH stretching. Langmuir and Freundlich adsorption isotherms were utilized to linearize the obtained data obtained from the batch experiment. The results revealed that the data fits perfectly to Langmuir isotherm but deviates slightly to Freundlich isotherm.

Acknowledgment

The authors wish to acknowledge San Roque Metals Inc. (SRMI) for funding this work, Material Science and Polymer Chemistry Laboratory for the material characterization, MinRes for the administrative support and the Division of Chemistry, Caraga State University for the use of instruments. Also, Mr. Wilfredo Amplayo and Ms. Ritchel Manansala deserve to be acknowledged for their technical assistance during the conduct of this study.

References

[1] Karade V C, Waifalkar P P, Dongle T D, Sahoo S C, Kollu P, Patil P S and Patil P B 2017 *Mater. Res. Express* **4** 096102
[2] Prasad C H, Gangadhara S and Venkateswarlu P 2016 *Appl. Nanosci.* **6** 797-802
[3] Yew Y P, Shameli K, Miyake M, Kuwano N, Ahmad Khairudin N B B, Mohamad S E B and Lee K X 2016 *Nanoscale Res. Lett.* **11** 276
[4] Monaliben S, Derek F, Shashi S, Suraj K T, Gerrard E and Jai P 2015 *Materials* **8** 7278-308
[5] Palaniyandi V, Govindarajan V K, Venkadapathi J, Jayabrata D and Raman P 2016 *Toxicol. Res.* **32** 95-102
[6] Ramesh A V, Lavakusa B, Satish Mohan B, Pavan Kumar Y, Ramadevi D and Basavaiah K 2017 *IOSR J. Appl. Chem.* **10** 35-43
[7] Sadia S, Arifa T and Yongsheng C 2016 *Nanomaterials* **6** 209
[8] Silveira C, Shimabuku Q L, Silva M F and Bergamasco R 2017 *Environ. Technol.* **39** 2926-36
[9] Yew Y P, Shameli K, Miyake M, Nurul Ahman Khairundin N B B, Mohamad S E B, Naiki T and Lee K X 2018 *Arabian J. Chem.* In Press, DOI: 10.1016/j.arabajc.2018.04.013
[10] Debadin B and Someswar C 2016 *Appl. Nanosci.* **6** 895-901
[11] Parashar U K, Kumar V, Bera T., Saxena P S, Nath G, Srivastava S K, Giri R and Srivastava A 2011 *Nanotechnol.* **22** 415104

[12] Caroling G, Priyadharshini M N, Vinodhini E, Ranjitham A M and Shanthi P 2015 *Int. J. Pharm. Bio. Sci*. **5** 25-43
[13] Santhoshkumar T, Rahuman A A, Jayaseelan C, Rajakumar G, Marimuthu S, Vishnu Kirthi A, Velayutham K, Thomas J, Venkatesan J and Kim S K 2014 *Asian Pac. J. Trop. Med.* **7** 968-76
[14] Raunak S, Subramani K, Petchi M R, Subbiah A K, Rangaraj S and Venkatachalam R 2018 *Prog. Org. Coat.* **124** 80-91
[15] Cempel M and Nikel G 2006 *Pol. J. Environ. Stud.* **15** 375-82
[16] Mcllveen W D and Negusanti J J 1994 *Sci. Total Environ.* **148** 109-38
[17] Mines and Geosciences Bureau Regional Office No. XIII, April 2018
[18] Wang X, Guo Y, Yang L, Han M, Zhao J and Cheng X 2012 *J. Environ. Anal. Toxicol*. **2** 154
[19] Mailoa M N, Mahendradatta M, Laga A and Djide N 2013 *Int. J. Sci. Technol. Res.* **2** 106-10
[20] Karamac M 2009 *Int. J. Mol. Sci.* **10** 5485-97
[21] Song C, Wu S, Cheng M, Tao P, Shao M and Gao G 2014 *Sustainability* **6** 86-98
[22] Omri A and Benzina M 2012 *Alexandria Eng. J.* **51** 343-50
[23] Mahmoud A M, Ibrahim F A, Shaban S A and Youssef N A 2015 *Egypt. J. Petrol.* **24** 27-35
[24] Shahzad A, Miran W, Rasool K, Nawaz M, Jang J, Lim S R and Lee D S 2017 *RSC Adv.* **7** 9764
[25] Simeonidis K, Kaprara E., Samaras T, Angelakeris M, Pliatsikas N, Vourlias G, Mitrakas M and Andritsos N 2015 *Sci. Total Environ.* **535** 61-8
[26] Purzamani H R, Mengelizadeh N, Jalil M and Moosavian Z 2017 *J. Environ. Health Sustain. Dev.* **2** 187-95
[27] Bulut Y and Zeki T E Z 2007 *J. Environ. Sci.* **19** 160-6
[28] Igwe J C and Abia A A 2007 *Ecletica Quim. Sao Paulo* **32** 33-42